Mediterranean precipitation climatology, seasonal cycle, and trend as simulated by CMIP5

Colin Kelley, Lamont-Doherty Earth Observatory, Columbia University, 61 Route 9W, Palisades, NY 10964

Mingfang Ting, Lamont-Doherty Earth Observatory, Columbia University, 61 Route 9W, Palisades, NY 10964

Richard Seager, Lamont-Doherty Earth Observatory, Columbia University, 61 Route 9W, Palisades, NY 10964

Yochanan Kushnir, Lamont-Doherty Earth Observatory, Columbia University, 61 Route 9W, Palisades, NY 10964

Corresponding author: Colin Kelley

phone: 828-335-4680

fax: 845-365-8736

email: ckelley@ldeo.columbia.edu

Abstract

Winter and summer Mediterranean precipitation climatology and trends since 1950 as simulated by the newest generation of global climate models, the Coupled Model Intercomparison Project phase 5 (CMIP5), are evaluated with respect to observations and the previous generation of models (CMIP3) used in the Intergovernmental Panel on Climate Change Fourth Assessment Report. Observed precipitation in the Mediterranean region is defined by wet winters and drier summers, and is characterized by substantial spatial and temporal variability. The observed drying trend since 1950 was predominantly due to winter drying, with very little contribution from the summer. However, in the CMIP5 multimodel mean, the precipitation trend since 1950 is evenly divided throughout the seasonal cycle. This may indicate that in observation, multidecadal internal variability, particularly that associated with the North Atlantic Oscillation (NAO), dominates the wintertime trend. An estimate of the observed externally forced trend shows that winter drying dominates in observations but the spatial patterns are grossly similar to the multi-model mean trend. The similarity is particularly robust in the eastern Mediterranean region, indicating a radiatively forced component being more robust there. Results of this study also reveal modest improvement for the CMIP5 multi-model ensemble in representation of the observed winter and summer climatology. The results of this study are important for assessment of model predictions of hydroclimate change in the Mediterranean region, often referred to as a “hotspot” of future subtropical drying.

1. Introduction

As a subtropical region, the Mediterranean region is expected to dry as a consequence of rising concentrations of greenhouse gases (GHG) [*IPCC,* 2007, *Hoerling et al.,* 2012]. As a thermodynamic consequence of increasing the atmospheric temperature, wet areas are expected to get wetter and dry areas, such as the subtropics, drier [*Held and Soden,* 2006; *Seager et al.,* 2007, 2010]. For the current century, the CMIP3 multimodel ensembles predicted a significant drying trend for the Mediterranean region [*IPCC*, 2007]. This "thermodynamic" subtropical drying is coupled with increasing precipitation in higher latitudes and circulation changes, primarily an expanding Hadley Cell and a poleward shift in the midlatitude storm tracks [*Lu et al.,* 2007; *Wu et al.,* 2010]. Even in the absence of any future changes in interannual variability, the long-term drying of the Mediterranean will lead to an increase in the likelihood of severe dry years, which would have important consequences for water resource in many Mediterranean countries, especially those already experiencing water insecurity. Whether a precipitation response to increasing radiative forcing has begun to emerge during recent decades, amid the often large natural interannual and multidecadal precipitation variability, is an open question, one that has been the subject of considerable debate [*Feldstein,* 2002; *Schneider et al.,* 2003; *Osborn,* 2004; *Kelley et al.,* 2011].

The previous generation of global climate models (GCMs) from the Coupled Model Intercomparison Project Three (CMIP3) was able to simulate the large-scale climatological features of Mediterranean region precipitation (see Figure 1). In the newest generation of global climate models, the CMIP5, in addition to other model advancements, increased spatial resolution potentially allows improved representation of the climatological pattern and amplitude associated with the complex physiography and orography of the region [*Giorgi and Lionello,* 2008]. With regard to the trend, the Mediterranean experienced a decline in precipitation since 1950 [*Hurrell et al.,* 2003; *Kelley et al.,* 2011], which could be the result of a combination of low frequency multidecadal variability and response to external forcing via increasing GHG [*Osborn,* 2004; *Kelley et al.,* 2011; *Mariotti and Dell'Aquila,* 2012; *Hoerling et al.,* 2012]. This study intends to address how well the CMIP5 models simulate the observed Mediterranean precipitation climatology, seasonal cycle and trends, and to what extent we can trust the multi-model mean trends as representing the externally forced trends.

2. Data and methods

2.1 Data

We use two high resolution (.5 degree by .5 degree) gridded datasets of observed precipitation over land, from the Climate Research Unit (CRU) version 3.1 [*NCAS BADC,* 2008] and the Global Precipitation Climatology Centre (GPCC) Full Data Product version 5 [*Schneider et al.,* 2008] and compare with CMIP3 [*Meehl et al.,* 2007] and CMIP5 [*Taylor et al.,* 2012) global climate models.

We use all available models from the CMIP3 and CMIP5 to create the multimodel means. In doing so we avoid any subjective bias associated with model selections. We use one run per model in forming the multimodel mean (MMM) to avoid bias toward any model. In the box plot, however, all model runs are included.

2.2 Methods

In order to make spatial intercomparisons possible, all datasets and model outputs were first linearly interpolated to a common $.5^{\circ}$ x $.5^{\circ}$ horizontal grid for the greater-Mediterranean region (10W - 50E, 20 - 60N). Due to the sparseness of observed station data prior to 1950 we perform all of the analysis with post 1950 data, with the exception of determining the external trend (detailed below). Trends are calculated via a linear least-squares fit to the time series at each grid point. For better comparison with observations, only precipitation over land is considered in this study.

As in *Kelley et al.*[2011], we employ a model-based S/N maximizing EOF analysis [*Allen and Smith,* 1997; *Venzke et al.,* 1999; *Chang et al.,* 2000; *Ting et al.,* 2009] to obtain the externally forced precipitation signal. The S/N maximizing EOF is first applied to CMIP5 multi-model ensemble (one run each) for 1900 to 2004 and using the corresponding models' preindustrial experiments to obtain the noise covariance. The gridded observed precipitation is then projected onto the S/N PC1 for the entire period (1900-2004) and the externally forced trend calculated from 1950-2004. More details of the method can be found in the supplementary material.

3. Precipitation Climatology

The six-month cold and warm season averaged (Nov-Apr and May-Oct, respectively), observed GPCC climatologies from 1950 to 2004 are shown in Fig. 1 (top panels). In the vicinity of the Mediterranean Sea, the majority of annual precipitation amounts fall during the six-month cold season, whereas over much of the rest of Europe, a substantial contribution comes from the summer half. The corresponding precipitation climatology for CMIP5 and CMIP3 multi-model means (MMMs) are shown in the middle and bottom panels of Fig.1. The coastal precipitation maximum in the winter half year is captured to some extent by the models, but at a much reduced amplitude. There are some improvements from CMIP3 to CMIP5 however, possibly due, in part, to the slightly enhanced spatial resolution in the recent generation models. As a result, the spatial pattern correlation between the observed and modeled fields increases slightly from CMIP3 (0.83) to CMIP5 (0.86). For the summer, the agreement is better between models and observations with spatial pattern correlations of 0.95 for CMIP5 and 0.94 for CMIP3. The better agreement between models and observations in summer is mainly due to drier conditions along the Mediterranean coasts compared to winter. As a comparison, the two gridded data sets, CRU and GPCC, are correlated at 0.94 for winter and 0.97 for summer (See Fig. A1 in the Supplementary Material). The Taylor diagram [*Taylor*, 2001] in Fig. A1 compares more closely the individual model's simulations of the precipitation climatologies in winter and summer.

To quantify the model spread and the seasonal cycle of the CMIP5 model simulated climatological rainfall, we show in Fig. 2 (left panels) the box and whiskers diagram for four selected regions, the entire Mediterranean region, the western, northern, and eastern Mediterranean (areas outlined in Fig.1a) for the four three-month seasons and the annual mean. The box edges indicate the 25% and 75% range of the model simulated climatological rainfall while the horizontal bar and red dot inside the box indicate the median and mean model rainfall, respectively, the two horizontal lines outside the box (whiskers) indicate the 5% and the 95% model range and the asterisks show the observed rainfall. A total of 109 model runs are used from 23 available CMIP5 models (see supplementary table A1) in Fig. 2. In all of the regions considered, the observed rainfall shows a clear seasonal cycle with maximum rainfall in the winter and minimum in summer, a characteristic of the Mediterranean climate. The CMIP5 models simulate the seasonal cycle reasonably well, but the majority of the models underestimate the winter maximum and overestimate the summer minimum, thus underestimating the amplitude of the seasonal cycle. The models show a larger spread in summer compared to other seasons, despite a higher spatial pattern correlation between MMMs and observations in summer. Overall, the climatological rainfall over the Mediterranean region is well simulated by the CMIP5 models. It is thus useful to reexamine the rainfall trends simulated in these models.

4. Precipitation Trends

The rainfall trends for the period from 1950 to 2004 in the CMIP5 models as compared to observations are summarized in the right panels of Fig. 2. For the entire Mediterranean region (top right), the mean and median of all models show a modest drying throughout the seasonal cycle with the largest drying trend in spring. But the observed trend shows a large seasonal cycle, ranging from a substantial drying in winter to a wetting trend in autumn. The winter observed rainfall trend for the 55 year period is larger than 95% of the model trends, with almost 10 mm/month reduction, or about 17% of the total winter season rainfall. For the rest of the seasonal cycle, the difference between the observed trend and the model mean trend is smaller, although autumn season precipitation shows a wetting trend outside of the middle half of the model predictions. The model underestimation of the observed winter drying comes mainly from the northern and western Mediterranean region and less so from the eastern Mediterranean.

The discrepancy between the models and observations in the autumn trend is dominated by the eastern Mediterranean region.

Kelley et al. [2011] examined the observed winter precipitation trends for the period 1960 to 2000 and determined the contribution to the total trend from the externally forced (estimated based on CMIP3 simulations) and the natural component (residual). They conclude that the externally forced trend is distinctive in its spatial pattern compared to the pattern of internal climate variability. The discrepancies between modeled and observed winter trends in Fig. 2 may indicate that the observed drying was dominated by multi-decadal variability rather than external radiative forcing. To confirm this, we show in Fig.3 the observed trend for 1950-2004 (left panels) for winter and summer half years. The winter observed trend shows a strong drying over western and northern Mediterranean, consistent with Fig.2, coupled with strong wetting trend in northern Europe. This pattern resembles the precipitation anomalies associated with the NAO [*Hoerling et al.,* 2012], thus suggesting the natural variability as a likely cause. The summer observed trend is weaker, and has a large wetting trend around and north of Black Sea. We follow the technique in *Kelley et al.* [2011] and estimate the externally forced precipitation trend due to radiative forcing using the signal to noise maximizing EOF PC1 obtained from the CMIP5 multi-model ensemble for the period 1900 to 2004 (see supplementary material for details). The estimated GPCC externally forced trend for the winter and summer half years, constructed based on the S/N PC1 (Fig.A2), are shown in the middle panels of Fig. 3. There is still a substantial amount of observed precipitation reduction surrounding the Mediterranean sea in the cold season, although with reduced amplitude compared to the total trend. The close resemblence between the observed total and external trends, however, suggest that the method of estimating the external trend is not able to remove entirely the trend associated with the NAO-related multi-decadal precipitation variability. The externally forced drying over the eastern Mediterranean, however, is more clearly seen in Fig.3c than in the total trend, indicating a more likely external cause. The summer observed external trend, while showing a consistent pattern of drying in most of the Mediterranean coasts, exhibits a much weaker amplitude throughout the region than its winter counterpart. The most significant observed drying in summer occurs south and east of the Black Sea, in Turkey.

The CMIP5 MMM trend pattern (right panels in Fig. 3) shows a much weaker drying throughout the Mediterranean region (notice the reduced color scale) compared to the observations, consistent with Fig. 2. There is a general agreement between the observed and modeled winter trends in that both have maxima in the western and eastern Mediterranean coasts. However, the maximum over the northern coasts is largely missing from the MMMs. For the summer half year, while the amplitude of the MMM trend is smaller than observed, the difference in amplitude between MMM trend and observed trend is not nearly as large as in winter. There is a reasonable correspondence between model and observations in summer drying over Turkey. Over Portugal and Spain, the MMM has a stronger drying trend in summer compared to observations.

It is interesting that the best agreement between CMIP5 MMM trends and the observed trends in both half years is in the eastern Mediterranean region (Fig.3). This is also true in Fig.2, where the eastern Mediterranean observed trend is closer to the model mean than any of the other regions. This indicates that the eastern Mediterranean may have the most significant externally forced drying trend. The greenhouse forcing of the eastern Mediterranean drying is also implicated in *Hoerling et al.* [2012], where they show that a global uniform warming of sea surface temperature can lead to strong eastern Mediterranean warming. The eastern Mediterranean is also a region of great water stress, for example in Turkey and Syria, and the future drying due to greenhouse warming will inevitably further deteriorate the water availability.

5. Summary

Using the newest global climate models from the new CMIP5 collection, we show that the Mediterranean precipitation climatology is generally well simulated in both spatial pattern and seasonal cycle. All models simulate the winter maximum and summer minimum in precipitation but the model mean and median slightly underestimate the amplitude of the seasonal cycle. There is a modest improvement of the CMIP5 climatology over CMIP3, possibly because of improved horizontal resolution.

In contrast, the Mediterranean precipitation trends of the last half century in the CMIP5 MMMs and the observations differ significantly, particularly in winter and over the northern Mediterranean region. The CMIP5 MMM trend indicates a modest drying throughout the seasonal cycle, with the strongest drying in the March, April and May spring season. The observed trend, on the other hand, shows a predominantly winter drying. It is not entirely clear what causes this discrepancy, although there is an indication that the strong observed winter drying may be due to multi-decadal natural variability [*Kelley et al.,* 2011). Our estimate of the externally forced trend in observations also shows a predominant winter drying over the region. There is a reasonable agreement in the spatial patterns of the CMIP5 MMM trend and the observed trend over the eastern Mediterranean region in both winter and summer.

The modest agreement in spatial patterns between modeled and the observed external trends leads us to further conclude that the radiatively forced portion of the precipitation trend has only begun to emerge relative to natural variability on multidecadal timescales, but that its influence is likely to grow in the future as the forcing increases. Future decreases in Mediterranean region precipitation brought on by global warming, even in the absence of any changes to the internal variability, will have important consequences, reinforcing the need for further research and better understanding of the mechanisms driving the region's hydroclimate. The CMIP5 model ensembles will likely prove a useful tool to this effect.

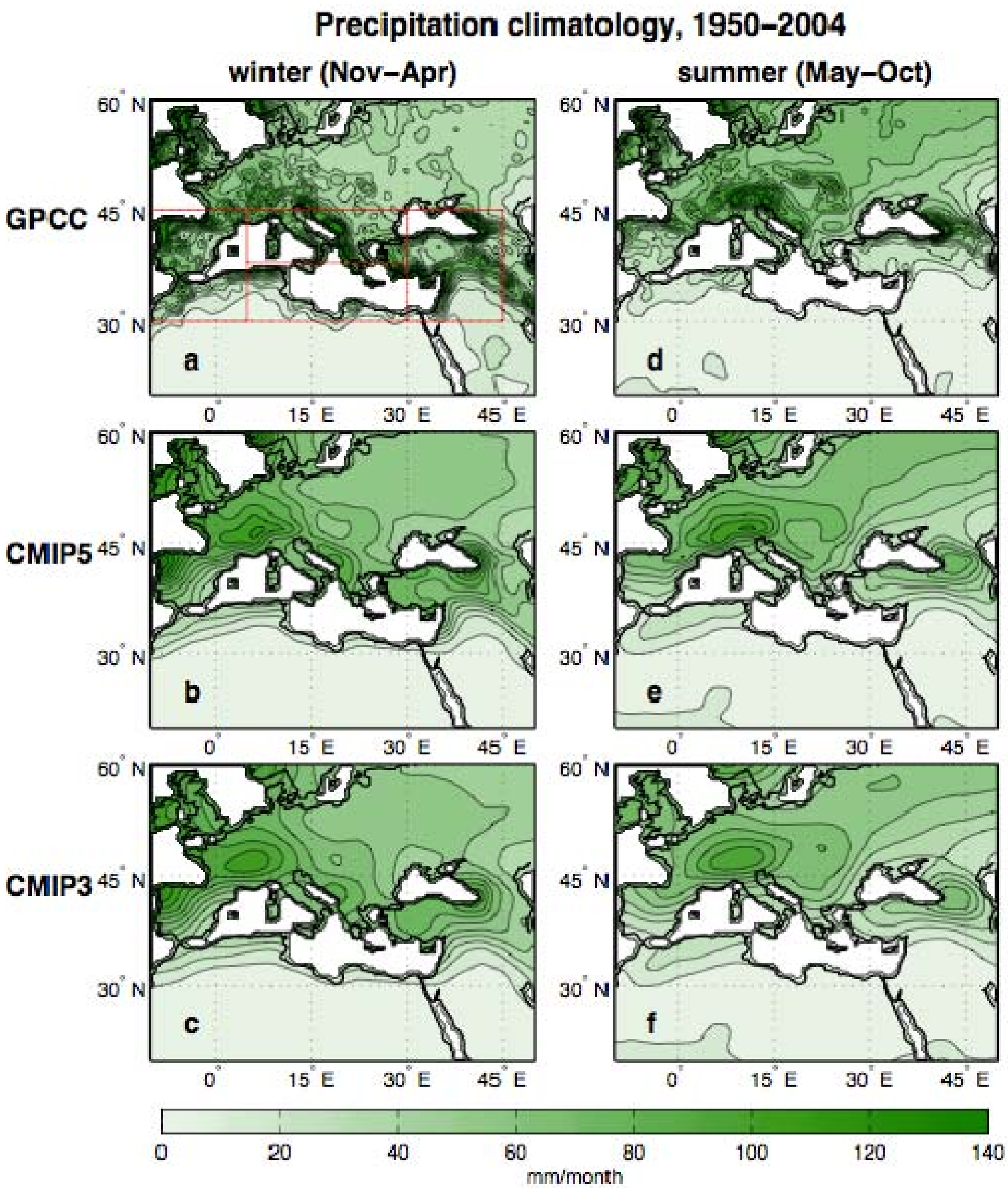

Fig. 1: Left, winter half (Nov-Apr) and right, summer half (May-Oct) precipitation climatology, 1950-2004, from the GPCC (top), CMIP5 multimodel mean (center) and CMIP3 multimodel mean (bottom). The red lines in (a) outline the region used in Fig. 2.

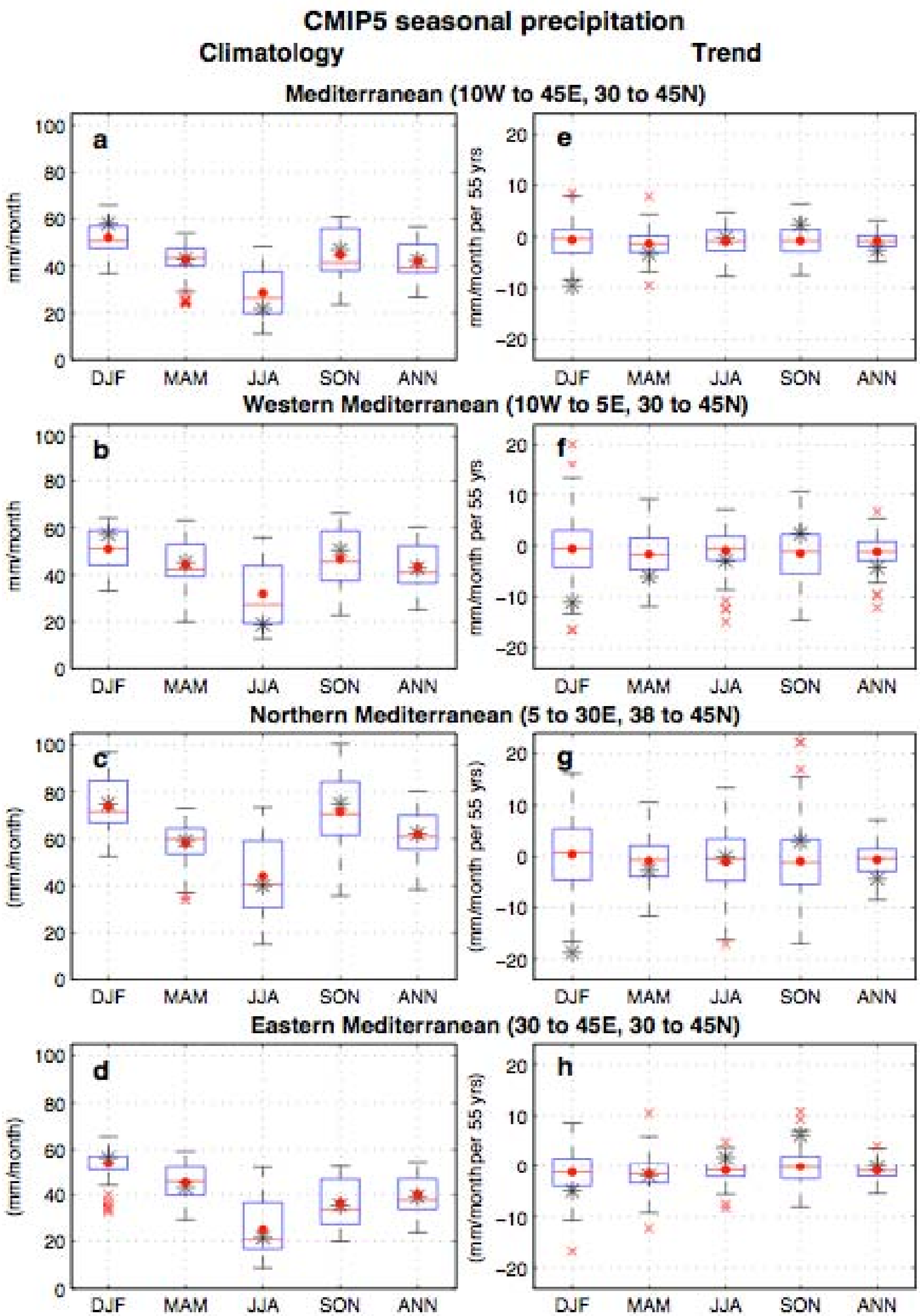

Fig. 2: Precipitation climatology (left) and trends (right) for 1950 to 2004 plotted as box and whisker diagrams using 109 historical runs from 23 CMIP5 models. The 25th and 75th percentiles of the model distributions are shown by the edges of the boxes, the medians and means are plotted as the horizontal lines and the red dots within the boxes respectively, the whiskers mark the 5th and 95th percentiles, and the red crosses indicate outliers. Observed values are indicated in black asterisks. Results are shown for the entire (a,e), western (b,f), northern (c,g) and eastern (d,h) Mediterranean region.

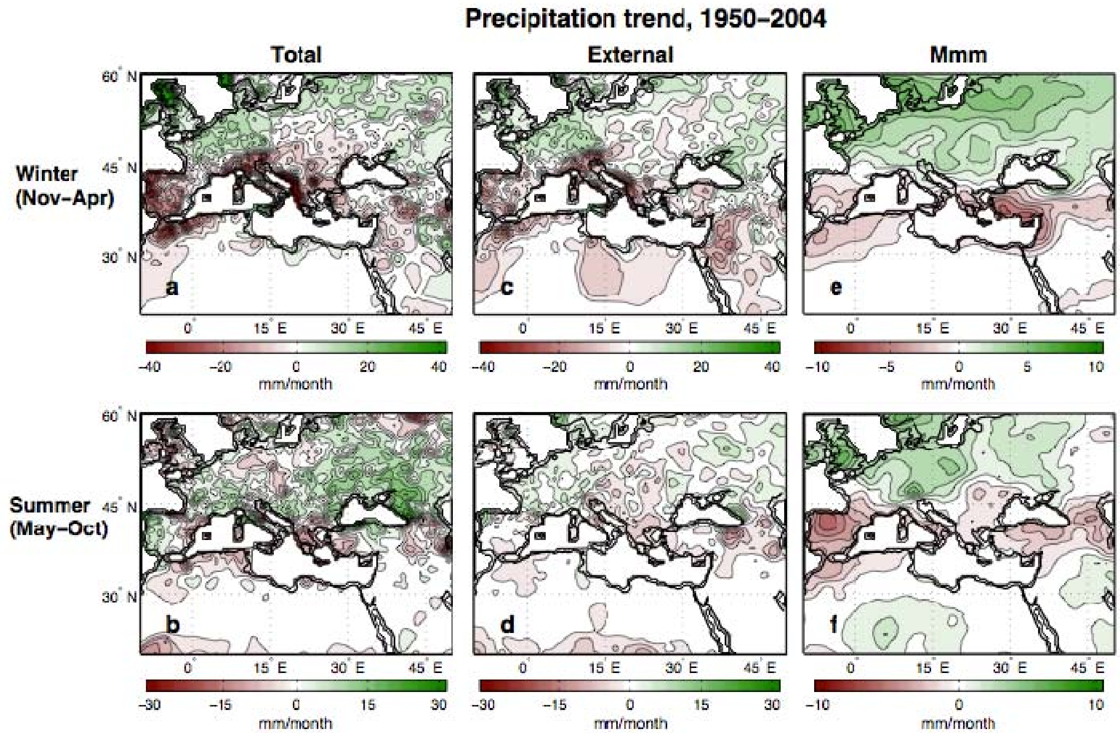

Fig. 3: Winter half (top) and summer half (bottom) GPCC precipitation total (left panels) and external (center panels) trend and CMIP5 multimodel mean (one run from each model) trend (right panels) for the 55 year period from 1950 to 2004.

Acknowledgements

The authors would like to thank the reviewers for their detailed and constructive comments, the Global Decadal Hydroclimate group at Lamont and Columbia for their input, and NOAA and NSF for support. This work is supported under the following grants: NA08OAR5320912, NSF RAPID project AGS-1128172, NOAA NA10OAR4310137, NSF AGS 08-04107 and NOAA NA08OAR4320912.

References

Blade, I., B. Liebmann, D. Fortuny and G. Jan van Oldenborgh (2011), Observed and simulated impacts of the summer NAO in Europe: implications for projected drying in the Mediterranean region. Climate Dyn., doi: 10.1007/s00382-011-1195-x

Chang, P., R. Saravanan, L. Ji and G. C. Hegerl (2000), The effect of local sea surface temperatures on atmospheric circulation over the tropical Atlantic sector. J. Climate, 13(13): 2195-2216.

Feldstein, S. B. (2002), The recent trend and variance increase of the annular mode. J. Climate, 15(1): 88-94.

Gillett, N., H. Graf, and T. Osborn (2003), Climate Change and the North Atlantic Oscillation. The North Atlantic Oscillation: Climatic Significance and Environmental Impact. e. a. J.W. Hurrell, Geophys. Mono., 134.

Giorgi, F. and P. Lionello (2008), Climate change projections for the Mediterranean region. Glob. Planet. Change, 63: 90–104

Held, I. M. and B. J. Soden (2006), Robust responses of the hydrological cycle to global warming. J. Climate, 19(21): 5686-5699.

Hoerling, M. P., J. Eischeid, J. Perlwitz, X. Quan, T. Zhang and P. Pegion (2012), On the Increased Frequency of Mediterranean Drought. J. Climate, 25: 2146-2161. doi: 10.1175/JCLI-D-11-00296.1

Hurrell, J. W., Y. Kushnir, G. Ottersen and M. Visbeck (2003), An overview of the North Atlantic Oscillation. The North Atlantic Oscillation: Climatic Significance and Environmental Impact. e. a. J.W. Hurrell, Geophys. Mono., 134: 1-35.

Kelley, C., M. Ting, R. Seager and Y. Kushnir (2011), The relative contributions of radiative forcing and internal climate variability to the late 20th Century winter drying of the Mediterranean region. Climate Dyn., 38(9-10): 2001-2015. doi: 10.1007/s00382-011-1221-z

Lu, J., G. A. Vecchi and T. A. Reichler (2007), Expansion of the Hadley cell under global warming. Geophys. Res. Lett., 34(6).

Mariotti A. and A. Dell’Aquila (2012), Decadal climate variability in the Mediterranean region: roles of large-scale forcings and regional processes. Climate Dyn. 38(5-6): 1129-1145, doi:10.1007/s00382-011-1056-7

Meehl, G. A., C. Covey, T. Delworth, M. Latif, B. McAvaney, J. F. B. Mitchell, R. J. Stouffer and K. E. Taylor (2007), The WCRP CMIP3 multimodel dataset - A new era in climate change research. B. Am. Meteorol. Soc., 88(9): 1383-94.

Osborn, T. J. (2004): Simulating the winter North Atlantic Oscillation: the roles of internal variability and greenhouse gas forcing. Climate Dyn., 22(6-7): 605-623.

Schneider, E. K., L. Bengtsson and Z. Z. Hu (2003), Forcing of Northern Hemisphere climate trends. J. Atmos. Sci., 60(12): 1504-1521.

Schneider, U., T Fuchs, A. Meyer-Christoffer and B. Rudolf (2008), Global precipitation analysis products of the GPCC. Global Precipitation Climatology Centre (GPCC), DWD, Internet publication: 1-12.

Seager, R., N. Naik and G.A. Vecchi (2010), Thermodynamic and Dynamic Mechanisms for Large-Scale Changes in the Hydrological Cycle in Response to Global Warming. J. Climate, 23(17): 4651-4668.

Seager, R., M. F. Ting, I. Held, Y. Kushir, J. Lu, G. Vecchi, H. Huang, N. Harnik, A. Leetma, N. Lau, C. Li, J. Velez and N. Naik (2007), Model projections of an imminent transition to a more arid climate in southwestern North America. Science, 316(5828): 1181-1184.

Solomon, S., D. Qin, M. Manning, Z. Chen, M. Marquis, K.B. Averyt, M. Tignor and H.L. Miller (eds.) (2007), IPCC, 2007: Climate Change 2007: The Physical Science Basis. Contribution of Working Group I to the Fourth Assessment Report of the Intergovernmental Panel on Climate Change: 996 pp.

Taylor, K. E. (2001), Summarizing multiple aspects of model performance in a single diagram. J. Geophys. Res., 106 (D7), 7183–7192, doi:10.1029/2000JD900719.

Taylor, K. E., R. J. Stouffer, and G. A. Meehl, An Overview Of CMIP5 And The Experiment Design, Bulletin of the American Meteorological Society, 93 (4), 485–498, 2012.

Thompson, D. W. J., S. Lee, and M.P. Baldwin (2003), Atmospheric processes governing the Northern Hempisphere Annular Mode/North Atlantic Oscillation. The North Atlantic Oscillation: Climatic Significance and Environmental Impact. e. a. J.W. Hurrell, Geophys. Mono., 134: 81-112.

Ting, M. F., Y. Kushnir, R. Seager and C. H. Li (2009), Forced and Internal Twentieth-Century SST Trends in the North Atlantic. J. Climate, 22(6): 1469-1481.

NCAS British Atmospheric Data Centre (2008), University of East Anglia Climatic Research Unit (CRU). [Phil Jones, Ian Harris]. CRU Time Series (TS) high resolution gridded datasets, [Internet]. Available from http://badc.nerc.ac.uk/view/badc.nerc.ac.uk__ATOM__dataent_1256223773328276

Venzke, S., M. R. Allen, R. T. Sutton and D. P. Rowell (1999), The atmospheric response over the North Atlantic to decadal changes in sea surface temperature. J. Climate, 12(8):

2562-2584.

Wu, Y., M. F. Ting, R. Seager, H. Huang and M. Cane (2010), Changes in storm tracks and energy transports in a warmer climate simulated by the GFDL CM2.1 model. Climate Dyn., 37(1-2): 53-72, doi: 10.1007/s00382-010-0776-4

Yin, J. H. (2005), A consistent poleward shift of the storm tracks in simulations of 21st century climate. Geophys. Res. Lett., 32(18).

Figure captions

Fig. 1: Left, winter half (Nov-Apr) and right, summer half (May-Oct) precipitation climatology, 1950-2004, from the GPCC (top), CMIP5 multimodel mean (center) and CMIP3 multimodel mean (bottom). The red lines in (a) outline the region used in Fig. 2.

Fig. 2: Precipitation climatology (left) and trends (right) for 1950 to 2004 plotted as box and whisker diagrams using 109 historical runs from 23 CMIP5 models. The 25th and 75th percentiles of the model distributions are shown by the edges of the boxes, the medians and means are plotted as the horizontal lines and the red dots within the boxes respectively, the whiskers mark the 5th and 95th percentiles, and the red crosses indicate outliers. Observed values are indicated in black asterisks. Results are shown for the entire (a,e), western (b,f), northern (c,g) and eastern (d,h) Mediterranean region.

Fig. 3: Winter half (top) and summer half (bottom) GPCC precipitation total (left panels) and external (center panels) trend and CMIP5 multimodel mean (one run from each model) trend (right panels) for the 55 year period from 1950 to 2004.

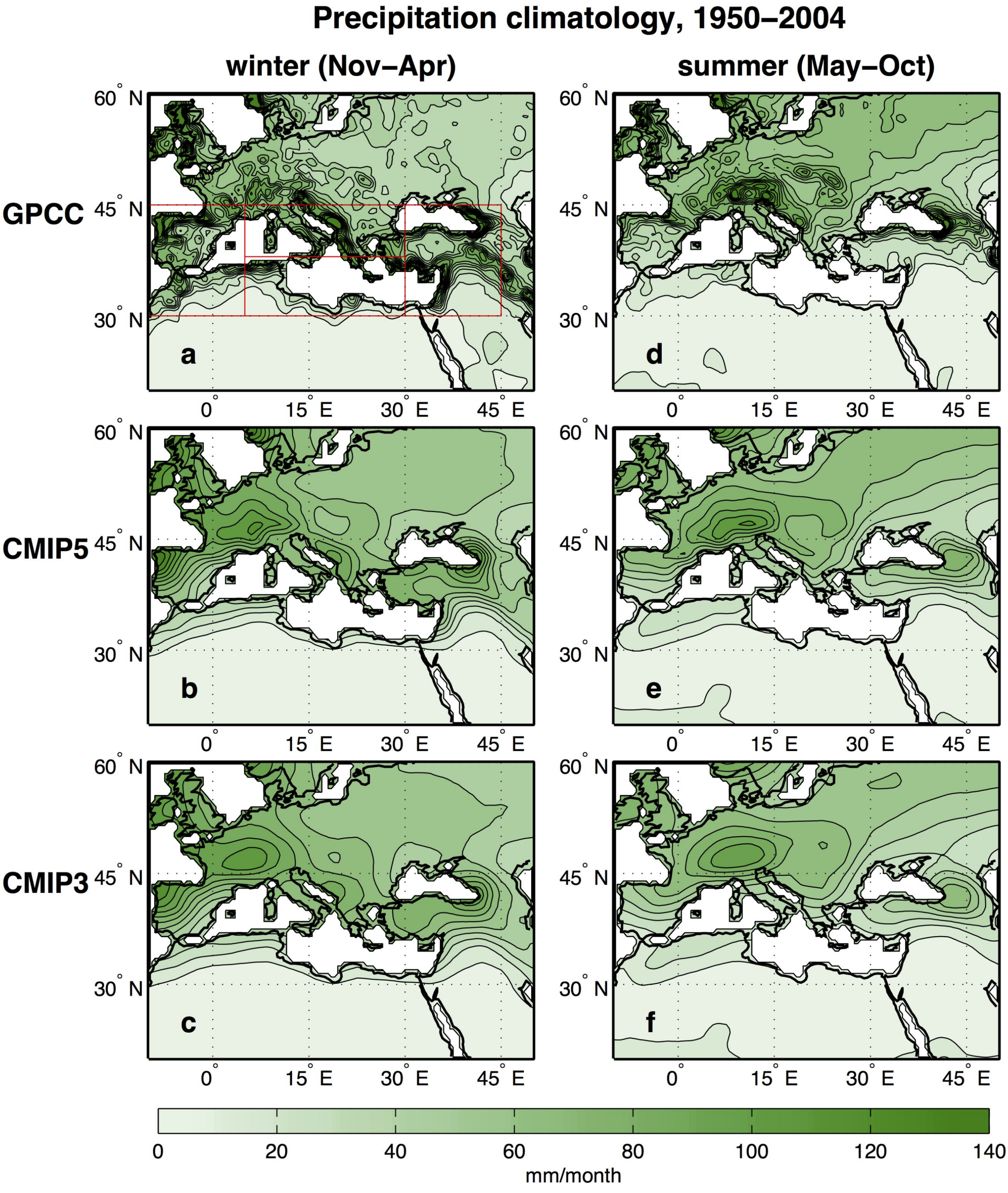

Precipitation climatology, 1950–2004
winter (Nov–Apr)
summer (May–Oct)
GPCC
CMIP5
CMIP3
60° N
45° N
30° N
0°
15° E
30° E
45° E
a
b
c
d
e
f
0
20
40
60
80
100
120
140
mm/month

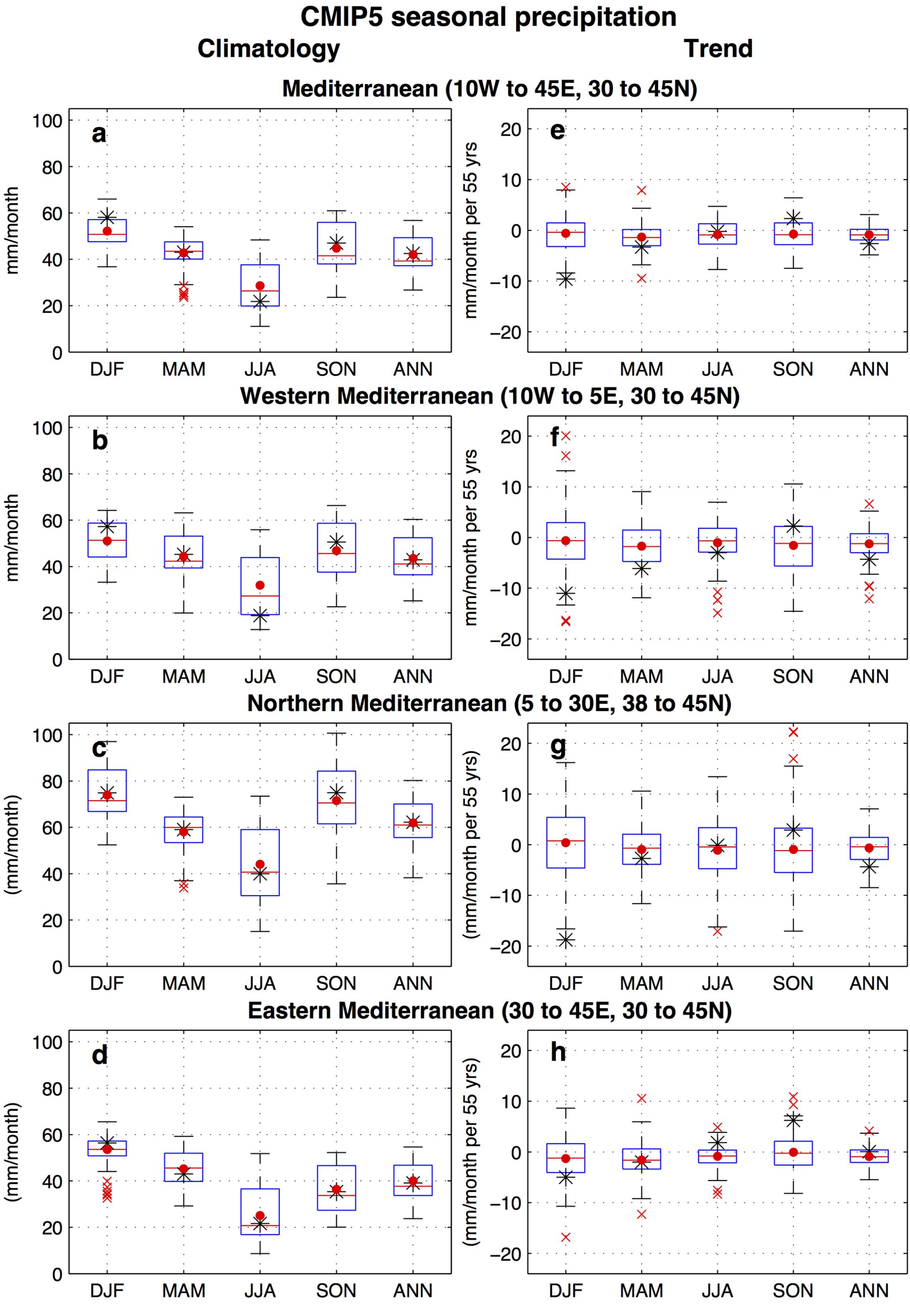

CMIP5 seasonal precipitation
Climatology
Trend
Mediterranean (10W to 45E, 30 to 45N)
Western Mediterranean (10W to 5E, 30 to 45N)
Northern Mediterranean (5 to 30E, 38 to 45N)
Eastern Mediterranean (30 to 45E, 30 to 45N)
a
b
c
d
e
f
g
h
mm/month
(mm/month)
mm/month per 55 yrs
(mm/month per 55 yrs)
DJF
MAM
JJA
SON
ANN
0
20
40
60
80
100
−20
−10
10

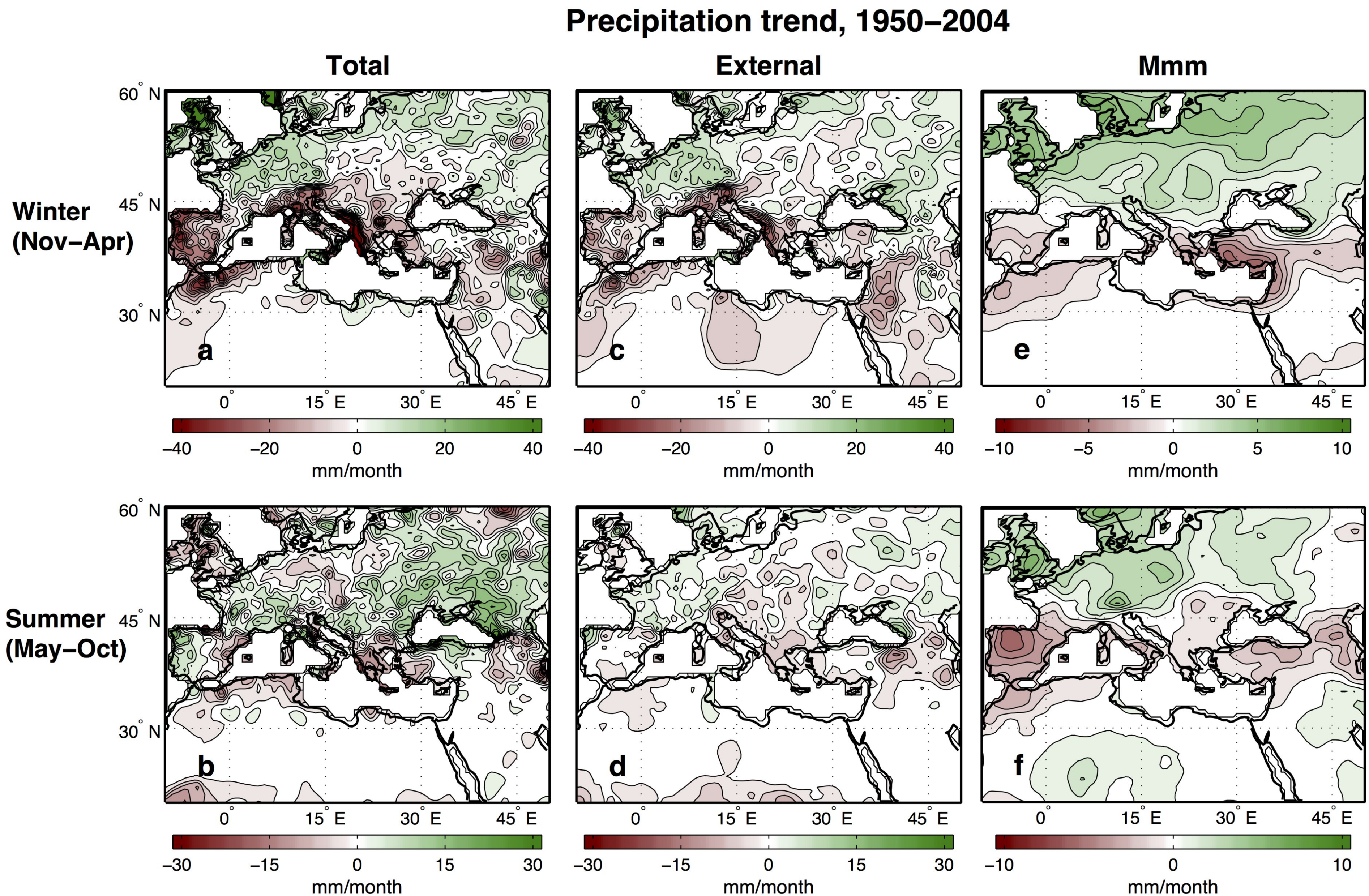

Precipitation trend, 1950–2004
Total
External
Mmm
Winter (Nov–Apr)
Summer (May–Oct)
60° N
45° N
30° N
0°
15° E
30° E
45° E
a
b
c
d
e
f
−40
−20
0
20
40
−30
−15
15
30
−10
−5
5
10
mm/month